PREPARED FOR THE U.S. DEPARTMENT OF ENERGY,
UNDER CONTRACT DE-AC02-76CH03073

PPPL-3522
UC-70

PPPL-3522

Generation of Plasma Rotation in a Tokamak by Ion-cyclotron Absorption of Fast Alfvén Waves

by

F.W. Perkins, R.B. White, P.T. Bonoli, and V.S. Chan

November 2000

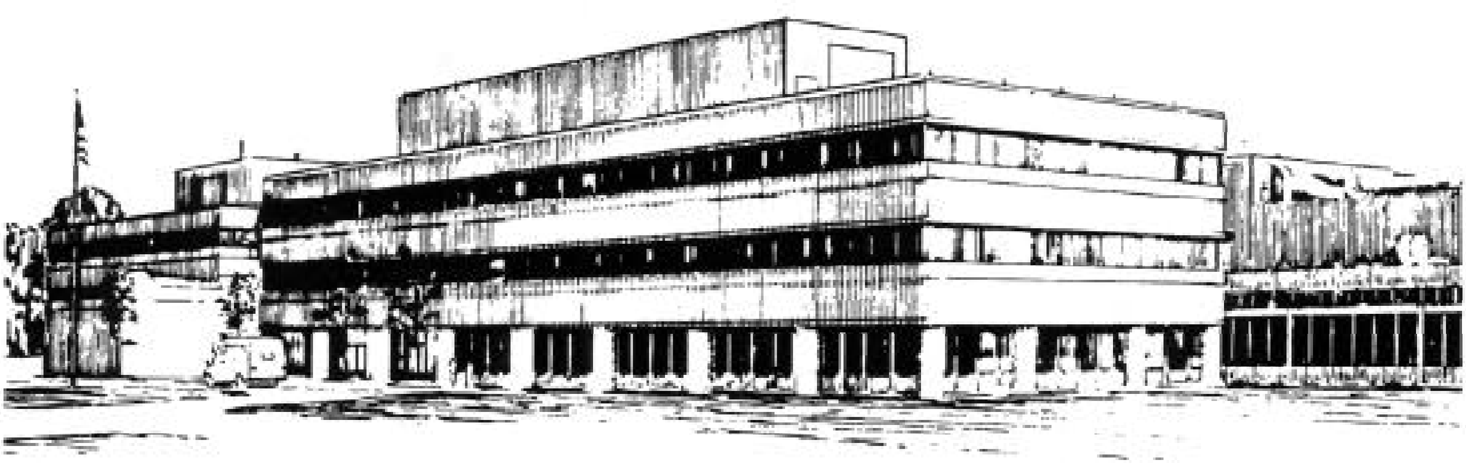

PRINCETON PLASMA PHYSICS LABORATORY
PRINCETON UNIVERSITY, PRINCETON, NEW JERSEY

Generation of Plasma Rotation in a Tokamak by Ion-Cyclotron Absorption of Fast Alfven Waves

F. W. Perkins[1,2], R. B. White[1,], P.T Bonoli[3], V. S. Chan[2]

[1] Plasma Physics Laboratory, PO Box 451, Princeton, NJ, 08543, USA
[2] General Atomics, PO Box 85608, San Diego, CA, 92186-5608,USA
[3] Plasma Science and Fusion Center, MIT, Cambridge, MA 02139-4307, USA

e-mail contact of main author: perkins@fusion.gat.com

Abstract. A mechanism is proposed and evaluated for driving rotation in tokamak plasmas by minority ion-cyclotron heating, even though this process introduces negligible angular momentum. The mechanism has two elements: First, angular momentum transport is governed by a diffusion equation with a no-slip boundary condition at the separatrix. Second, Monte-Carlo calculations show that ion-cyclotron energized particles will provide a torque density source which has a zero volume integral but separated positive and negative regions. With such a source, a solution of the diffusion equation predicts the on-axis rotation frequency Ω to be $\Omega = (4q_{max}W J^*)(eBR^3a^2n_e(2\pi)^2)^{-1}(\tau_M/\tau_E)$ where $|J^*| \approx 5\text{-}10$ is a nondimensional rotation frequency calculated by the Monte-Carlo ORBIT code. Overall, agreement with experiment is good, when the resonance is on the low-field-side of the magnetic axis. The predicted rotation becomes more counter-current and reverses sign on the high field side for a no-slip boundary. The velocity shear layer position is controllable and of sufficient magnitude to affect microinstabilities.

Introduction. How can a plasma develop an angular momentum content when none is supplied? Recent observations on the Alcator C-Mod [1,2] and JET[3] tokamaks of appreciable co-current central velocity appearing in response to minority ion-cyclotron fast-wave heating raise this question since minority ion-cyclotron heating is a negligible angular momentum source. This article proposes and evaluates a mechanism which can resolve this apparent conflict.

The physics of plasma rotation and the generation and transport of angular momentum density are interesting both as a fundamental physics process and as the basis for a plasma control tool. Review articles by Ida[4] and Chan[5] give a comprehensive account of radial electric field and plasma rotation observations as well as a detailed discussion of the interaction of radiofrequency heating methods with plasma rotation, respectively. Rotational response of plasmas to angular momentum input is observed to have a momentum confinement time τ_M

comparable to the observed energy confinement time τ_E (c.f. Sec. 4.2 of ref.4 and ref 6-8) and an angular momentum diffusivity profile similar to the anomalous heat diffusvity profile.

Indeed, plasma rotation is an effective method for optimizing magnetic fusion plasmas. Differential rotation increases the stability of large-scale distortions of the entire plasma as well as fine scale modes, which cause turbulent transport. In the case of turbulent modes, differential rotation breaks up their structure and prevents growth[9,10]. Large-scale modes acquire increased stability when, by differential rotation, magnetic distortions which are fixed in the frame of the rotating plasma appear as time-dependent fluctuations in the frame of a conducting shell which surrounds the plasma. Consequently, with sufficient differential rotation, these fluctuations can not penetrate the shell, increasing the maximum pressure that can be stably confined[11-12].

Alcator C-Mod observations[1,2,13,14] have further established that the central rotation velocity increases roughly linearly with the plasma energy content and that the rotation is strongly peaked toward the plasma center when the ion-cyclotron resonance is close to the magnetic axis. The rotation profile broadens as the cyclotron resonant surface moves to larger minor radius. The sense of rotation is co-current regardless of the location of the resonant surface with respect the magnetic axis, unless an internal transport barrier develops[13]. The co-current rotation reported[14] in ohmically-heated Alcator C-Mod plasmas lies outside the scope of this work but could possibly be understood in terms of a modification of the no-slip boundary condition introduced below.

This article proposes and evaluates a mechanism for core plasma rotation to develop in response to minority ion-cyclotron heating. The argument has two parts. First, it is assumed that angular momentum transport is governed by a diffusion equation that has a no-slip boundary condition at the separatrix and a torque density source term as discused below. If the torque-density source term has two separated regions, one with positive and the other with negative torque density, but is constrained to have zero volume-integrated torque, then the solution of the angular momentum diffusion equation will yield a finite central rotation rate. The physics picture is that angular momentum generated in the outer part of the plasma diffuses to the surface and is lost faster than that supplied to the inner part.

The second part of the argument rests on an evaluation of the torque density applied to the bulk plasma arising from the slowing down of ions accelerated by the minority-ion-cyclotron process. The cyclotron acceleration process itself introduces no angular momentum and leaves each particle's canonical angular momentum unchanged as well. The motivating physics picture is that, as a result of finite banana widths and collisions, a fast ion which is born on an initial magnetic surface will slow down and return to the bulk plasma over a distribution of magnetic surfaces. This constitutes localized radial currents in the fast particles. Neutralizing radial currents then flow in the bulk plasma and produce $j_r B_\theta R$ torque densities -- just the separated regions of torque density needed to drive rotation. However this simple picture must be augmented by collisional transfer of mechanical angular momentum from the fast particles to the bulk plasma, which is of the same magnitude as the $j_r B_\theta R$ torque density. Thus a precise calculation of all sources of torque density that rigorously accounts for angular momentum is required to determine whether torque density will be applied to the bulk plasma and to determine its sense. The Monte-Carlo code ORBIT [15,16] has been modified to rigorously acount for collisional momentum exchange between energetic particles and a bulk plasma as well as providing for stochastic energization by perpendicular energy diffusion.

The present work differs from previous theoretical models[17,18] in its rigorous accounting of angular momentum including all collisional transfer between the energetic and bulk plasma species, the role of radial currents associated with energetic-ion banana diffusion, and the use of a diffusive transport equation to describe plasma response to torques. As a result, profiles of rotation rate versus minor radius are available. Plasmas with direct momemtum input by orbit loss or electrode radial currents rotate as a consquence of finite net applied torque.

The manuscript first describes our models for fast wave propagation and ion-cyclotron heating. Next, we develop a solution to the angular momentum diffusion equation in general axisymmetric geometry that defines the integrated collisional and $j_r B_\theta R$ torque densities that the ORBIT code must compute. Additions to ORBIT for this work are summarized. Results give plasma rotation curves parametrized by location of the ion-cyclotron resonance. A discussion of their sensivity to input parameters, correspondence to experiment, and a conclusion follow.

Two-Component Plasma Model. The starting point for our model is to separate the plasma into two components: a high-energy tail created by minority ion-cyclotron heating whose evolution will be followed by the Monte-Carlo ORBIT code and a bulk plasma, which responds to applied torque density via a diffusive angular momentum transport equation with a model momentum diffusvity profile $\chi_M = a^2q^n/C_n\tau_M$ that spatially depends on q. Here τ_M denotes the momentum confinement time, which is taken comparable to the energy confinement time τ_E [5, 9]. The motivating physics comes from the observation that if one interprets the almost linear dependence of tokamak energy confinement time on a q-dependent diffusivity, then n≥2. We will focus on n=2 and for which $C_2 = 2(1+\kappa^{-2})\, q_{max}$ based on an analytic power balance model.

Fast Wave Propagation. An important aspect of fast wave heating is that refraction focuses the waves onto the magnetic axis region and continues to maintain high wave intensities near the midplane for major radius values less than the magnetic axis. Calculations by the TORIC code[19], portrayed in Fig. 1 illustrate this. Qualitatively, one can capture this aspect of fast wave heating by defining an intense wave region as portrayed in Fig. 1. Particles will undergo ion-cyclotron energization only if their orbits cross the cyclotron resonance surface within the intense wave region. This has the consequence of limiting the range of magnetic surfaces where ion-cyclotron heating can take place and generating regions of high rotational shear, especially when the cyclotron resonance lies to the high-field-side of the magnetic axis. The boundary $\pm z_o$ of the intense field region has been taken to be

$$z_o = \begin{cases} z_{max} & R - R_a < z_{max} \\ R - R_a & R - R_a > z_{max} \end{cases} \qquad (1)$$

with R_a the magnetic axis major radius and z_{max} = 7 cm for Alcator C-Mod example of Fig. 1.

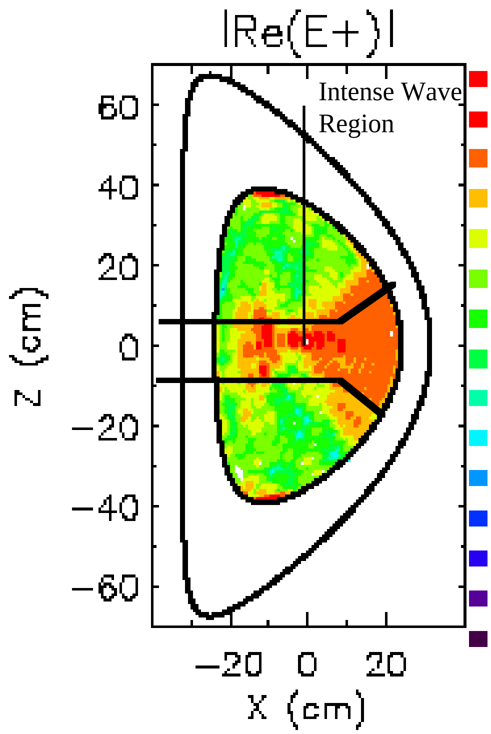

FIG. 1. Propagation of the fast wave in Alcator C-Mod when the ion-cylcotron resonance lies at -8 cm, well to the high-field-side of the magnetic axis. The toroidal mode number is n=10 is representative of the antenna spectrum.

Ion-Cyclotron Heating. Two models for ion-cyclotron heating have been used. Model 1 instantaneously energizes a particle from the bulk plasma to a specified energy E_o. This initial creation is rigorously constrained to introduce zero net angular momentum and zero canonical angular momentum change for each particle, as is appropriate for ion-cyclotron heating. It is effected by starting energetic particles with their banana tips lying on the cyclotron surface within the intense wave region. A distribution of off-midplane, banana-tip height with z, $dN/dz = \left(1-(z/z_o)^2\right)\left(2z_o - z^2\right)^{-1/2}$ is used so that only particles in the intense wave region illustrated in Figure 1 are created. The energetic ions are then followed until they lose all their energy by the Monte-Carlo ORBIT code[15,16] which includes ion-ion pitch-angle-scattering collisions[20] as well as ion and electron energy drag collisions. These collisions return energetic particles to the bulk plasma distributed over a region comparable to the banana full width about the originating magnetic surface. Our assumption that the fast waves transfer no net angular momentum to the energetic particles is rigorous for fast-waves with $k_{||} = n/R = 0$. For realistic values $n \approx \pm 10$, it can be shown that angular momentum input remains negligible for a balanced n-spectrum.

Ion-cyclotron Model 2 introduces ion-cyclotron heating by giving a particle a stochastic kick in perpendicular energy $\Delta E_\perp$ each time it passes through the cyclotron resonance surface. The kicks are given by

$$<(\Delta E_\perp)^2> = 2\, E_\perp\, Es \qquad <\Delta E_\perp> = Es \tag{2}$$

where

$$E_s = c_\perp \frac{4\pi\, \nu_o q\, R_c\, E_o\, M_p^{1/2}}{\left[2(E - E_\perp) + T\right]^{1/2}} \frac{F(z)\, \alpha_c}{\left(\alpha^2 + \alpha_c^2\right)^{1/2}} \quad . \tag{3}$$

We note that equal changes in E and $E_\perp$ leave $v_\|$ and the canonical angular momentum unchanged. Therefore this operator introduces no angular momentum. The quantity Es is constructed to have properties expected of ion-cyclotron heating. In particular, the mean square energy kick should be proportional to $E_\perp$, inversely proportional to $\mathbf{v}_\|\cdot\mathbf{R}/R$, be limited to the strong wave region, and have the rate of energy increase for a particle injected at energy E_o comparable to its loss of energy via coulomb collisions. Thus, E_s, as given in Eq.(3), is a function of R_c, z, ν_o, E, $E_\perp$, q, Eo, and T — all evaluated at the cyclotron resonance crossing point. The adjustable constant $c_\perp$ governs the energy input via ICRF heating to be large, but not very large, compared to the initial particle parameter $\nu_o E_o$. It is expected that $c_\perp$ will be close to unity. The parameter $\alpha = \alpha(R_c, z) = \mathbf{R}\cdot\phi\times\nabla\psi(R\,\nabla\psi)^{-1}$ depends only on magnetic surface geometry and reflects the degree of tangency between the magnetic surface and the cyclotron resonant surface. An ad-hoc cutoff at $\alpha_c = 0.1$ prevents mathematical divergences. The formula for F(z) describes the strong field region

$$F(z) = \sqrt{2}\left(1 - \frac{z^2}{z_o^2}\right)\left(2 - \frac{z^2}{z_o^2}\right)^{-1/2} \tag{4}$$

With this model, initial particle parameters are a monoenergetic, isotropic velocity distribution at energy E_o and are distributed uniformly in space for $\Phi(R_c,0) < \Phi < \Phi(R_c, z_o)$. This initial condition introduces zero angular momentum. Again, particles are followed by ORBIT until they reach zero energy. This model is closer to actual ion-cyclotron heating, but produces a bias rotation, which we discuss and correct for below.

Angular Momentum Diffusion. The general, steady-state axisymmetric angular momentum transport equation equates angular momentum flux through a flux surface to the torque generated inside that surface.

$$\oint \mathbf{dl} \times \boldsymbol{\phi} \cdot \hat{\nabla}\, \Phi\, 2\pi\, R^3\, n\, M\, (\chi_o q^n)\, \frac{\partial \Omega}{\partial \Phi} \;=\; -\,T(\Phi)\, \dot{N}\, M\, R_a{}^2\, \Omega_a \qquad (5)$$

where Φ denotes the area enclosed by a magnetic surface in the poloidal plane and serves as the independent flux-surface label. Here Ω denotes the angular rotation rate, which must be constant on a flux surface, and T(Φ) is the nondimensional integrated torque-per-particle exerted on the plasma inside magnetic surface Φ and is computed by ORBIT. The fundamental mass, length, and frequency units used by ORBIT are the proton mass, the major radius , and the ion-cyclotron frequency, both evaluated at the magnetic axis. $\dot{N}$ denotes the rate at which particles are supplied and is related to the applied power through $\dot{N}\, E = P$ where E is the average net energy-per-particle transferred from the energetic particles to the bulk plasma. For ion cyclotron Model 1, $E=E_o$.

We will neglect variations of R and the effective diffusivity $\chi_o q^n$ on a magnetic surface. Equation (5) can then be recast as

$$\frac{1}{\dot{N}}\, \frac{\partial \Omega}{\partial \Phi} \;=\; -\, \frac{T(\Phi)\, \Omega_a}{8\pi^2\, \Phi\, H(\Phi)\, n\, R\, \left(\chi_o q^n\right)} \qquad (6)$$

where H(Φ) is defined by

$$4\pi\, \Phi\, H(\Phi) \;=\oint \mathbf{dl} \times \boldsymbol{\phi} \cdot \hat{\nabla}\, \Phi = \int\, dA\;\; \nabla^2\Phi \qquad (7)$$

where the integral is over the area inside the magnetic surface. It can be shown that H(Φ) is a surface function, will be close to unity, and depend only weakly on the shape of the magnetic surface. Therefore, the expression for the rotation rate becomes

$$\frac{1}{\dot{N}}\left(\Omega(\Phi)\; - \Omega(\Phi_{max})\right) \;=\left(\frac{\Omega_a}{8\pi^2\, n\, R\, \chi_o}\right) \int_{\Phi}^{\Phi_{max}} \frac{T(\Phi)\, d\Phi}{\Phi\, q^n} \quad . \qquad (8)$$

The integrated torque will also have a surface contribution when particles are being lost from the plasama. The requirement for zero angular momentum input is $T(\Phi_{max}) = 0$. Equation (8) computes the rotation rate from the Integrated Torque T. Angular momentum conservation requires $T(\Phi_{max}) = 0$. A simple q-profile is employed $q = 1+(q_{max}-1)\cdot(\Phi/\Phi_{max})$.

The physics rationale for a surface no-slip boundary condition $\Omega(\Phi_{max}) = 0$ derives from the property of ideal MHD that axisymmetric equilibria must have Ω a function of flux-surface only combined with the observation that the separatrix flux surface is line-tied to a fixed conducting material boundary and so can not rotate. In reality, the complex and strong radial electric fields found in the H-mode pedestal[21] may well alter the boundary condition from that of simple ideal MHD considerations· Observation of rotation in Ohmic H-modes[14] are consistent with this picture.

Since the principal contribution to the integral for Ω is expected to come from a thin layer whose thickness scales with the gyroradius, this integral will be rescaled by a factor v^{-1}, where $v = (2E/M)^{1/2}(R_a\omega_{ci})^{-1}$. We also introduce T^* via $T = \dot{N}T^*v$, where $\dot{N}$ is the rate at which is the rate at which the plasma heating is supplying energetic particles of energy E so the fast-wave heating power $P = \dot{N}E$. T^* has the interpretation of being the angular momentum transferred from an average energetic particle to the bulk plasma inside flux surface Φ in units of $(2EM)^{1/2}R_a$. Thus, the expression for the rotation rate becomes

$$\frac{\Omega(\Phi) - \Omega(\Phi_{max})}{\dot{N}} = \frac{v^2}{2(2\pi)^2\langle n\chi_o\rangle} I_n^*(\Phi) \qquad I_n^*(\Phi) = \frac{1}{v}\int_{\Phi}^{\Phi_{max}} \frac{d\Phi'}{\Phi' q^n} T^*(\Phi') \ . \tag{9}$$

Numerical results reported below will confirm that, with this scaling, I^* is insensitive to particle energy.

ORBIT Calculations of Integrated Torque. Equation (9) reduces our problem to the calculation angular momentum driven in the bulk plasma by the ensemble average of individual particles. The complex evolution of particle orbits, with pitch angle scattering transforming orbits from trapped to passing and back again, suggests the use of a Monte-Carlo method. The ORBIT code[15,16] , which follows particle banana and passing orbits and their evolution by collisions[20] , while strictly conserving angular momentum, has been adapted to this problem.

The ORBIT code follows an ensemble of Monte-Carlo particles with the initial condition as specified in the preceding paragraph as their orbits evolve under the influence of collisions. The collision model is ion-ion pitch angle scattering and energy drag of minority ions against a cold bulk deuterium plasma and electrons, as given by

$$\frac{1}{E}\left(\frac{dE}{dt}\right) = -2\nu_o \left(\frac{E_o}{E}\right)^{3/2} \left\{\frac{M_p}{M_d} + \frac{4}{3\sqrt{\pi}}\left(\frac{m_e}{M_p}\right)^{1/2}\frac{E^{3/2}}{T^{3/2}}\right\} \qquad d\langle\theta^2\rangle / dt = \nu_o\left(E_o / E\right)^{3/2} \quad (10)$$

where $\nu_o = 2\pi\sqrt{2}n_e e^4 \ell n\Lambda\, M_p^{-1/2}E_o^{-3/2}$ and E_o is the initial particle energy.

ORBIT records the angular momentum increment $MR(\Delta v_{\|})$ [in units of $(2ME)^{1/2}R_a$] received by a Monte-Carlo particle in each collision event as well as the magnetic surface on which the collision took place. An equal but opposite angular momentum increment is then accumulated in one of the 10,000 computational bins in toroidal flux corresponding to the magnetic surface where the collision occured. From this data one forms $T_2^* = \int_0^\Phi MR\Delta v_{\|} d\Phi$, which is the Monte-Carlo ensemble average angular momentum impulse imparted to the bulk plasma within flux surface Φ by collisions with energetic particles.

Torque also arises from the radial curents which result when a particle comes to rest on a magnetic surface which differs from their originating one. It is straight foward to show that the total torque δT exerted on a shell of thickness $\delta\psi$ in poloidal flux is given by the radial current I_r. The radial current is determined in turn by the fraction of particles which come to rest inside a given magnetic surface. For each Monte Carlo particle, the ORBIT code records the initial magnetic flux surface Φ_o and its final position is assigned to one of the bins. From this data one can form

$$T_1^* = \frac{1}{v}\int_0^\Phi \frac{d\Phi'}{q}\, G(\Phi') \qquad G(\Phi) = \begin{cases} F(\Phi) & \Phi < \Phi_o \\ 1 - F(\Phi) & \Phi > \Phi_o \end{cases} \qquad (10)$$

and $F(\Phi)$ is the the average number of particles whose final position is inside surface Φ. T_1^* is the angular momentum given to the bulk plasma by a single ensemble-average particle through Rj_rB_θ torques [in units of $(2ME)^{1/2}R_a$] . The discontinuity in $G(\Phi)$ arises from subtraction of a cold bulk particle in the initial conditions.

Lastly, when particles are lost from the plasma, they carry with them their mechanical angular momentum which is accumulated as T_3^*. At the plasma surface the total integrated torque $T_1^* + T_2^*\ T_3^*$ is evaluated and found to vanish with a relative accurracy of $2\cdot10^{-3}$ or better. Thus, our physics and computational scheme does not introduce any angular momentum.

This completes our formalism. Monte Carlo runs determine $F(\Phi)$, $T_1^*(\Phi)$, $T_2^*(\Phi)$, and finally $I^*(\Phi)$. Because our final expression involves two integrations over the distributions in computational bins, the results are very insensitive to the number of bins and adequate accuracy results from 1000 Monte Carlo particles per run.

Results. Non-dimensional rotation integrals I_2* for a scan of resonance surface locations are presented for a circular tokamak model for Alcator C-Mod, based on ion-cyclotron Model 1 which starts particles at an energy of 48 keV with their banana tips on the cyclotron resonance surface in the intense wave region. The magnetic axis lies at $R_{c\,=}$ 67 cm and q_{max} = 4.0. Calculations done with an initial energy of 24 keV and with different initial pitch confirmed insensivity to input parameters except resonance location. Fig. 2 displays the results. One notes the following features: The magnitude of the central rotation is $|I_2^*|$ = 5-10. The rotation profiles are small outside the cyclotron resonance surface (except for R=51 which had appreciable lost particles). And, the sense of rotation changes from co-current to counter-current as the resonance surface passes through the magnetic axis.

Ion cyclotron Model 2, with perpendicular energy diffusion, has a potential for bias arising from its initial conditions. This arises from the results of calculations in which starting energetic particles in pairs of equal but opposite parallel velocity resulted in driving a rotation. Although contributions from a range of major radius values produce an approximate cancellation, a residual rotation remains. Consequently, we compute the difference between rotation profiles of a reference case without ICRF heating and a case with the same initial conditions, but with ICRF. We then form

$$J_2^* = \frac{E_o}{E_{ICRF} - E_o}\left(I_2^*{}_{ICRF} - I_2^*{}_{Ref}\right) \qquad (11)$$

which gives the incremental rotation normalized by the incremental energy, which is the difference between the starting energy and the total average energy transferred by a particle to the bulk plasma. Fig. 3 presents results for an initial energy of 10 keV and $c_\perp$ = 1.0, which resulted in a modest increase of particle energy due to ICRF heating.

It is evident that these two models produce effectively equivalent rotation profiles.

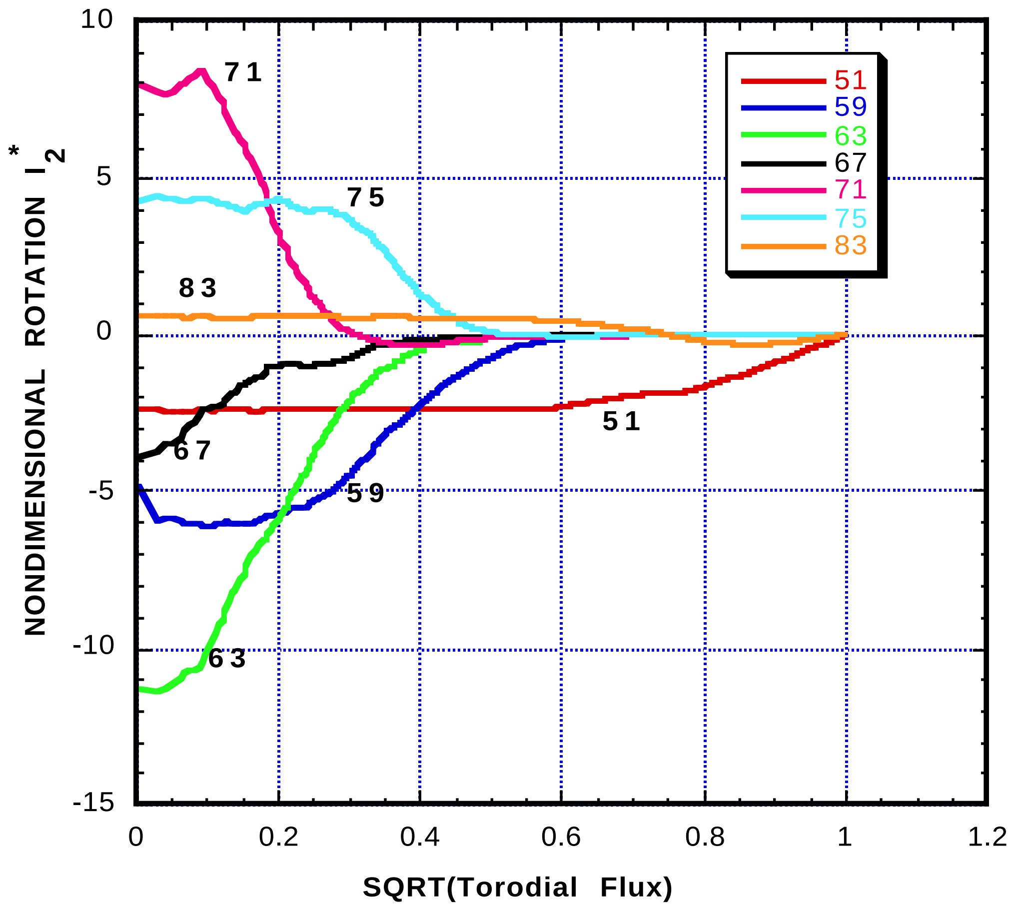

FIG. 2. Nondimensional rotation profiles I_2^* for ICRF Model 1 versus square root of normalized toroidal flux for various values of the major radius of cyclotron resoance surface. Magnetic axis is R = 67 cm

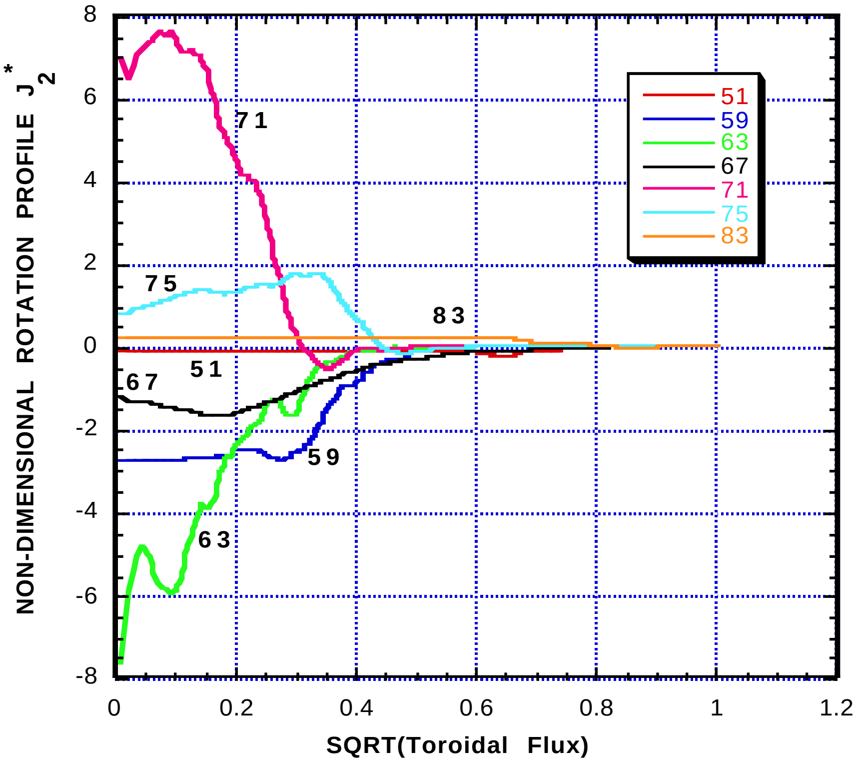

FIG. 3. Nondimensional Rotation profiles J_2^* for ion-cyclotron model 2 with the major radius of cyclotron resonance layer as a parameter.

Fig.4 presents the integrated torque profiles T_1^* and T_2^* for R= 71cm. It is evident that the co-current torque by collisional mechanical angular momentum transfer is what generates the co-current rotation. This plot attests to the accuracy of the ORBIT code in attaining zero integrated torque at the plasma boundary.

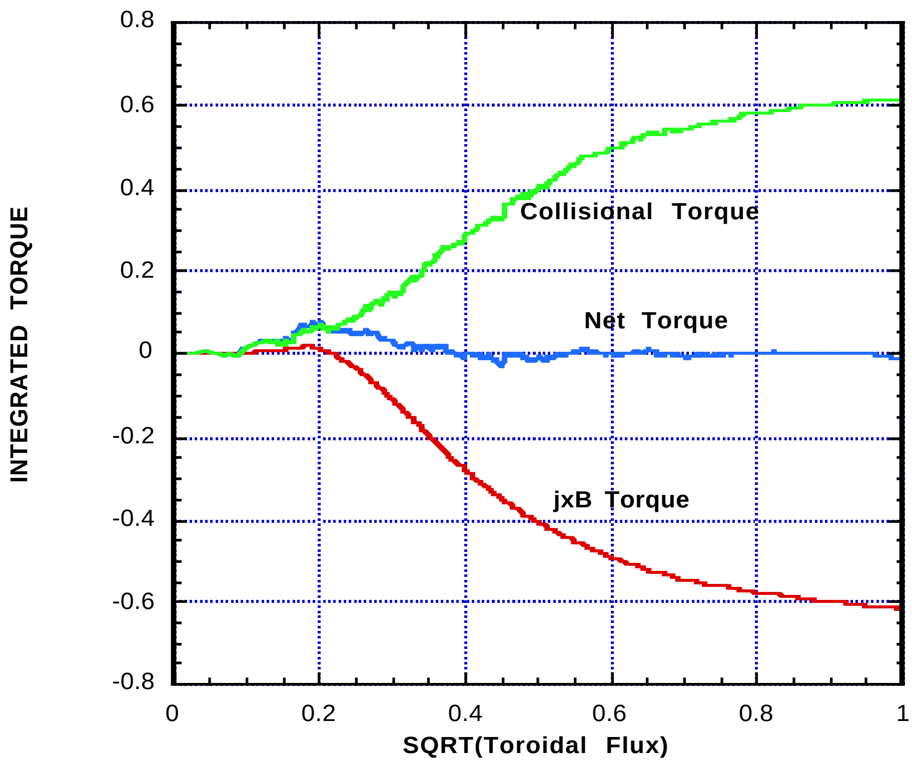

FIG. 4 Integrated torque for ICRF model 1 at R= 71 cm.

Putting the results into dimensional form, the rotational profile takes the form

$$\Omega - \Omega_{boundary} = \frac{4\, q_{max}\, W}{eBR^3 a^2 n_e\, (2\pi)^2} \left(\frac{\tau_M}{\tau_E} \right) I_2^* \qquad (14)$$

where W denotes plasma energy content. Based on $I_2^* \approx 8$ and $n_e = 3 \cdot 10^{20} m^{-3}$, Eq.(16) gives a central rotation rate of 110 kilorads/s, which is the observed rate in Alcator C-Mod, for the no-slip boundary condition $\Omega_{boundary} = 0$.

Lets us also note that off-axis resonance locations (cf R=59 cm,75 cm) produce layers of high velocity shear that are strongly localized. The velocity shear values are roughly $8 \cdot 10^5$Hz for C-Mod parameters, are comparable to drift wave frequencies (less than 10^6 Hz), and therefore should be effective at stabilizing drift waves and producing internal transport barriers.

Conclusion. Overall, we can conclude that a physics mechanism exists for ICRF heating to be an effective free energy source which creates torque densities that can generate core rotation and velocity shear, when coupled with diffusive transport of angular momentum. Quantitative agreement is obtained between theory and experiment. when the resonance lies on the low-field-side of the magnetic axis. Key predictions are: 1) that the sense of plasma rotation changes becoming more counter-current for resonant surfaces on the high-field-side of the magnetic axis and 2) that the plasma rotation profile is flat outside the neighborhood of the cyclotron resonant magnetic surface. Velocity shear layers near cyclotron resonant surfaces are sufficiently intense to affect microinstability turbulence. The surface boundary condition remains a source of uncertainty. We note that the physics of this problem with complex particle orbits changing from ciculating to trapped and back again needs a computational solution to attain a reliable result. We have benefitted from discussions with C. S. Chang, J. Rice, M. Porkolab, and Y. Omelchenko. This work was supported by US DOE Contract DE-AC0276CH03073.

References

[1] J. E.Rice *et al.*, Nuclear Fusion **38** 75 (1998).

[2] J. E. Rice et al., Nuclear Fusion **39** 1175 (1999).

[3] L,-G. Eriksson, E. Righi, and K.-D. Zastrow, Plasma Phys Controlled Fusion **39**, 27 (1997)

[4] K. Ida, Plasma Phys. Controlled Fusion **40** (1998) 1429.

[5] V. Chan, *et al.*, in Radio Frequency Power in Plasmas 1999 (American Institue of Physics) 45.

[6] R. J. Hawryluk,, *et. al.* Plasma Phys. Control. Fusion **33** 1509 (1991) .

[7] K. Burrell, *et. al.* Nuclear Fusion **28** 3 (1988).

[8] S. D. Scott, *et al.* Phys. Rev. Lett. **64**, 531 (1990).

[9] K. Burrell, *et al.* Phys. Plasmas **4** 1499 (1997).

[10] R. E. Waltz, *et al.,* Phys. Plasmas **5** 1784 (1998).

[11] M. S.Chu, *et al.,* Phys. Plasmas **2** 2236 (1995).

[12] T. S. Taylor, *et al.* Phys. Plasmas **2** 2390 (1995).

[13] J. E. Rice, *et al.*, in Proc. of 18th IAEA Fusion Energy Conf. (Sorrento,2000)

[14] I. H. Hutchinson, *et al.*, Phys. Rev. Lett. **84** 3330 (2000).

[15] R. B. White, R.B., Phys. Fluids B **2** 845 (1990).

[16] R. B. White and , M.S.Chance Phys. Fluids **27** 2455 (1984).

[17] C. S. Chang *et al.*, Phys. Plasmas **6** 1969 (1999).

[18] C. S. Chang *et al.*, Phys.Plasmas **7** 1089 (2000)

[19] M. Brambilla, Nuclear Fusion **38** (1998) 1805.

[20] A. H. Boozer and G. Kuo-Petravic, Phys. Fluids **25** (1981) 851.

[21] K. Burrell, Phys. Plasmas **6** 4418 (1999).

External Distribution

Plasma Research Laboratory, Australian National University, Australia
Professor I.R. Jones, Flinders University, Australia
Professor João Canalle, Instituto de Fisica DEQ/IF - UERJ, Brazil
Mr. Gerson O. Ludwig, Instituto Nacional de Pesquisas, Brazil
Dr. P.H. Sakanaka, Instituto Fisica, Brazil
The Librarian, Culham Laboratory, England
Library, R61, Rutherford Appleton Laboratory, England
Mrs. S.A. Hutchinson, JET Library, England
Professor M.N. Bussac, Ecole Polytechnique, France
Librarian, Max-Planck-Institut für Plasmaphysik, Germany
Jolan Moldvai, Reports Library, MTA KFKI-ATKI, Hungary
Dr. P. Kaw, Institute for Plasma Research, India
Ms. P.J. Pathak, Librarian, Insitute for Plasma Research, India
Ms. Clelia De Palo, Associazione EURATOM-ENEA, Italy
Dr. G. Grosso, Instituto di Fisica del Plasma, Italy
Librarian, Naka Fusion Research Establishment, JAERI, Japan
Library, Plasma Physics Laboratory, Kyoto University, Japan
Research Information Center, National Institute for Fusion Science, Japan
Dr. O. Mitarai, Kyushu Tokai University, Japan
Library, Academia Sinica, Institute of Plasma Physics, People's Republic of China
Shih-Tung Tsai, Institute of Physics, Chinese Academy of Sciences, People's Republic of China
Dr. S. Mirnov, TRINITI, Troitsk, Russian Federation, Russia
Dr. V.S. Strelkov, Kurchatov Institute, Russian Federation, Russia
Professor Peter Lukac, Katedra Fyziky Plazmy MFF UK, Mlynska dolina F-2, Komenskeho Univerzita, SK-842 15 Bratislava, Slovakia
Dr. G.S. Lee, Korea Basic Science Institute, South Korea
Mr. Dennis Bruggink, Fusion Library, University of Wisconsin, USA
Institute for Plasma Research, University of Maryland, USA
Librarian, Fusion Energy Division, Oak Ridge National Laboratory, USA
Librarian, Institute of Fusion Studies, University of Texas, USA
Librarian, Magnetic Fusion Program, Lawrence Livermore National Laboratory, USA
Library, General Atomics, USA
Plasma Physics Group, Fusion Energy Research Program, University of California at San Diego, USA
Plasma Physics Library, Columbia University, USA
Alkesh Punjabi, Center for Fusion Research and Training, Hampton University, USA
Dr. W.M. Stacey, Fusion Research Center, Georgia Institute of Technology, USA
Dr. John Willis, U.S. Department of Energy, Office of Fusion Energy Sciences, USA
Mr. Paul H. Wright, Indianapolis, Indiana, USA

The Princeton Plasma Physics Laboratory is operated
by Princeton University under contract
with the U.S. Department of Energy.

Information Services
Princeton Plasma Physics Laboratory
P.O. Box 451
Princeton, NJ 08543

Phone: 609-243-2750
Fax: 609-243-2751
e-mail: pppl_info@pppl.gov
Internet Address: http://www.pppl.gov